

**THE TALE OF PYROXENE IN MESOSIDERITE ASUKA 09545, INFERRED FROM TWO GENERATIONS OF EXSOLUTION LAMELLAE.** L. Pittarello<sup>1</sup>, S. J. McKibbin<sup>2</sup>, A. Yamaguchi<sup>3</sup>, J. Gang<sup>4,5</sup>, D. Schryvers<sup>4</sup>, V. Debaille<sup>6</sup>, and Ph. Claeys<sup>7</sup>, <sup>1</sup>Department of Lithospheric Research, University of Vienna, Vienna, Austria (lidia.pittarello@univie.ac.at), <sup>2</sup>Geowissenschaftliches Zentrum, Isotopengeologie, Georg-August-Universität Göttingen, Göttingen, Germany (seann.mckibbin@gmail.com), <sup>3</sup>National Institute of Polar Research (NIPR), Tachikawa, Japan, <sup>4</sup>Electron Microscopy for Materials Science (EMAT), University of Antwerp, Antwerp, Belgium, <sup>5</sup>Unité Matériaux et Transformations, Université de Lille, France, <sup>6</sup>Laboratoire G-Time, Université Libre de Bruxelles, Brussels, Belgium, <sup>7</sup>Analytical, Environmental, and Geo-Chemistry (AMGC), Vrije Universiteit Brussel (VUB), Brussels, Belgium.

**Introduction:** Mesosiderites consist of a breccia containing roughly equal amount of metal and silicate (e.g., [1,2]), interpreted as a mixture of basaltic material from the crust and metal from the core of two differentiated parent bodies [3] or even from mixing within the same parent body [4,5]. The metal portion metal has recorded the slowest cooling rate from ca. 550°C ever measured in the Solar System (e.g., [6]). The formation processes of mesosiderites are still debated. In particular, the cooling history of the silicate fraction in mesosiderite is not completely unraveled, so far, although most of the estimates agree that silicate cooling rate was fast until ca. 800°C [7-9].

Here a study of pyroxene from mesosiderite Asuka (A) 09545, collected in Antarctica during a joint Belgian-Japanese mission [10], is presented. Two generations of exsolution lamellae, investigated by electron microprobe and transmission electron microscopy, allow the evaluation of the thermal history experienced by this pyroxene. By comparison with data in the literature, the implications in the cooling rate of silicates in mesosiderites will be addressed.

**Methods:** A petrographic thin section and a polished chip of A 09545 were used. Scanning electron microscopy (SEM) was performed with a FEI Inspect S50 instrument, equipped with an energy-dispersive spectrometry (EDS) detector, at the Royal Belgian Institute of Natural Science, and with a JEOL 6400 at the Vrije Universiteit Brussel, Brussels, Belgium. For analysis of the detailed chemical composition of the pyroxene, a JEOL JXA-8200 electron microprobe, equipped with five wavelength-dispersive spectrometers (WDS) and one EDS, was used at the NIPR, Tachikawa, Japan. Image analysis for quantitative petrography has been applied on back scattered electron (BSE) SEM images, using the free software ImageJ. Site-specific transmission electron microscopy (TEM) foils were prepared with a FEI Helios NanoLab 650 dual beam system (Field Emission-FE-SEM and focused ion beam-FIB) by Ga<sup>+</sup> ion sputtering. The foils were then analyzed with a Philips CM20 TEM, operated at 200 kV and equipped with a Nanomegas "Spinning Star" precession unit and

an Oxford INCA x-sight EDS detector. Both instruments are located at the EMAT laboratory of the University of Antwerp, Belgium. Additional optical microscopy was performed at the Natural History Museum of Vienna, Austria, on selected thin sections of mesosiderites from the local collection.

**Results:** A 09545 consists of a clast-supported breccia, with gabbroic clasts and amoeboid metal (ca. 20-30 vol%). Silicate clasts contain, in order of abundance, pyroxene, anorthitic plagioclase (An<sub>91</sub>), chromite, apatite, and minor amount of free silica. No clastic matrix is observed, likely completely recrystallized, therefore A 09545 can be classified as B3, according to the classification by [4] and [11].

All pyroxene crystals, independent of their size, exhibit two generations of exsolution lamellae (Fig. 1a). The pyroxene host has composition Wo<sub>3</sub>En<sub>59</sub>Fs<sub>38</sub> and diffraction pattern consistent with monoclinic "ferrosilite", space group P2<sub>1</sub>/c. Thus it can be considered clinoenstatite. Exsolution lamellae 1 (lam 1) develop roughly parallel to cleavage, have average thickness of 20-30 µm, composition Wo<sub>42</sub>En<sub>41</sub>Fs<sub>17</sub> and the diffraction pattern of monoclinic high-Ca pyroxene (space group C2/c). Composition and crystallography are consistent with augite. Exsolution lamellae 2 (lam 2) are contained within lam 1 and organized in subparallel sets. Lam 2 have average thickness lower than 300 nm, with regular spacing of ca. 900 nm, orientation parallel to [001], composition Wo<sub><1</sub>En<sub>56</sub>Fs<sub>43</sub>, as determined by standardless EDS-TEM measurements, and diffraction pattern consistent with that of clinoenstatite (space group P2<sub>1</sub>/c).

#### Discussion:

**Geothermobarometry.** The equilibrium between host and the first exsolution (lam 1 + lam 2) yields 946-1028°C at ca. 2-24 Kbar, and between lam 1 and lam 2 681-809°C, assuming Ca content 0.1 wt%, consistently with instrumental detection limit (geothermobarometers by [12] and [13]). These estimates are consistent with the graphical evaluation based on [14].

**Cooling rate.** Several parameters support a relatively slow cooling rate of pyroxene to generate

such an exsolution pattern, including lamellae orientation and symmetry class [15-17]. Only single crystal diffraction would provide a definitive evaluation of the cooling rate of pyroxene (e.g., [18]), but the presence of inclusions and the fine grain size hamper the applicability of this method in the investigated sample.

The presence of clinoenstatite, as host and as lam 2, rather than orthoenstatite, might suggest that cooling was relatively rapid between the two exsolution events at 946-1028°C and 681-809°C. The host pyroxene probably followed the metastable extension of the pigeonite field down through the high pigeonite C2/c to low pigeonite P2<sub>1</sub>/c transition (Wo<sub>3</sub> in Fig. 1b).

*Frequency of occurrence of exsolution lamellae in pyroxene in mesosiderites.* Inverted pigeonite with exsolution lamellae along two orientations should be common in the sub-group 3 mesosiderites [11], but this feature is observed also in Vaca Muerta, a type 1 mesosiderite [19]. Inverted pigeonite is relatively common in mesosiderites, but two generations of exsolution lamellae and the occurrence of monoclinic low-Ca pyroxene seems to be quite rare. However, in most previous works, orthopyroxene might have been reported without checking the actual symmetry class. According to [20], a range of cooling rates were experienced by mesosiderites in their parent body after the reheating event, due to different burial depths in the parent body. This might explain the observed differences among mesosiderites. However, the formation and the preservation of the described exsolution lamellae would require either slow cooling after pigeonite crystallization or reheating with peak temperature lower than 550°C for mesosiderite A 09545.

**Conclusions:** The occurrence of two generations of exsolution lamellae in pyroxene from mesosiderite A 09545 sheds new light on the cooling history of the silicate fraction in mesosiderites. Our findings support a relatively slow cooling for pyroxene in A 09545 or at least a limited reheating event, to grant the preservation of the fine-grained lamellae. The rarity of occurrence of the described features in pyroxene reflects the variety of features exhibited by mesosiderites and points to different thermal histories and origins of the silicate component of mesosiderites.

**Acknowledgements:** Study funded by BELSPO, FWO, and FWF.

**References:** [1] Prior G. T. (1918) *Min Mag* 18:151-172 [2] Rubin A.E. and Mittlefehldt D.W. (1992) *GCA* 56:827-840. [3] Wasson J. T. and Rubin A. E. (1985) *Nature* 318:168-170. [4] Mittlefehldt D.W. et al. (1998) In *Planetary materials*, edited by Papike J. J. Washington D.C.: Mineralogical Society of America. pp. 4:1-4:195. [5] Scott E.

R. D. et al. (2001) *MAPS* 36:869-881. [6] Hopfe W. D. and Goldstein J. I. (2001) *MAPS* 36:135-154. [7] Delaney J. S. (1983) *Meteoritics* 18:289-290. [8] Ruzicka A. et al. (1994) *GCA* 58:2725-2741. [9] Ganguly J. et al. (1994) *GCA* 58:2711-2723. [10] Yamaguchi A. et al. (2014). *Meteorite Newsletter* 23, NIPR, Japan. [11] Powell B.N. (1971) *GCA* 35:3-34. [12] Putirka K. D. (2008) In: Putirka, K., Tepley, F. (Eds.), *Minerals, Inclusions and Volcanic Processes, Reviews in Mineralogy and Geochemistry*, Mineralogical Soc. Am., v. 69, pp. 61-120. [13] Brey G. P. and Köhler T. (1990) *J Petrol* 31:1353-1378. [14] Lindsley D.H. (1983) *Am Min* 68:477-493. [15] Nakazawa H. and Hafner S.S. (1977) *Am Min* 62:79-88. [16] Robinson P. et al. (1977) *Am Min* 62:857-873. [17] Grove T. L. (1982) *Am Min* 67:251-268. [18] Molin G. et al. (2006) *EPSL* 128:479-487. [19] Rubin A. E. and Jerde E. A. (1987) *EPSL* 84:1-14. [20] Sugiura N. and Kimura M. (2015) *LPSC XLVI*, Abs. # 1646. [21] Whitney D. L. and Evans B. W. (2010) *Am Min* 95:185-187.

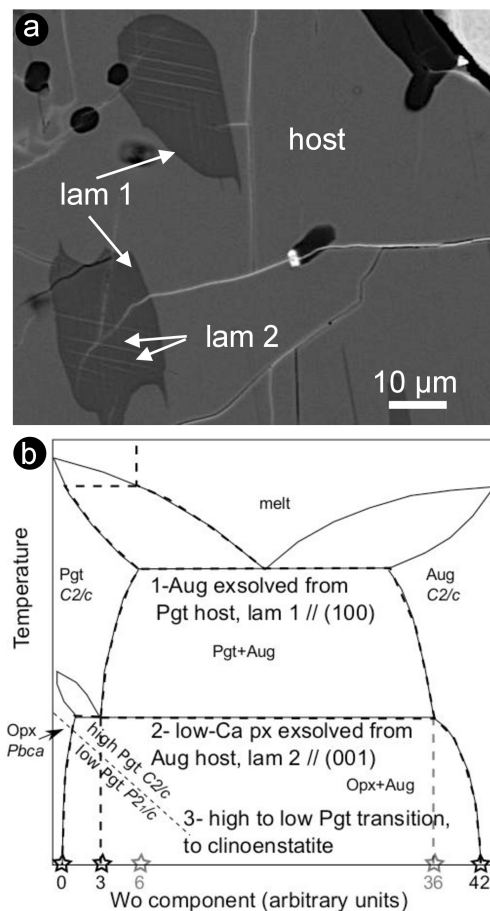


**Fig. 1.** Exsolution lamellae in pyroxene. a) BSE-SEM image showing the host pyroxene, lam 1 and lam 2. b) Simplified phase diagram for pyroxene at low pressure. The dashed line represents the evolution of pyroxene in the investigated sample. Mineral abbreviations according to [21].